Electronic structure of Ga-, In-, and Tl-doped PbTe: A supercell study of the impurity bands

Khang Hoang* and S. D. Mahanti†
Department of Physics and Astronomy, Michigan State University, East Lansing, Michigan 48824, USA
(Received 31 January 2008; revised manuscript received 16 June 2008; published 11 August 2008)

The physics of deep defect states associated with group-III (Ga, In, Tl) impurities in PbTe has been of great interest over the last several decades. Three different models have been proposed to understand interesting and unusual properties exhibited by these impurities. These are "impurity level" model, "mixed-valence" model, and "autocompensation" model. Recent studies that were carried out using *ab initio* density-functional theory and supercell models give a detailed microscopic picture of the deep defect states associated with these impurities. The computed single-particle electronic density of states does not support the mixed-valence model where the impurities are supposed to be in 3^+ and 1^+ charge states, rather it is in favor of the impurity level model. In this paper, we present a detailed analysis of the impurity bands, impurity levels in the dilute limit, and the hybridization between the impurity level and the host PbTe bands. We find that the impurity level overlaps the conduction band (In), is in the gap (Ga), and overlaps the valence band (Tl). The possibility of the autocompensation model where impurities in charge states 1^+ and 1^- coexist (a different type of mixed valency) is briefly discussed.

DOI: 10.1103/PhysRevB.78.085111 PACS number(s): 71.55.−i, 71.20.−b, 71.28.+d

I. INTRODUCTION

The nature of deep defect states in narrow-band-gap semiconductors with large electronic dielectric constants such as PbTe has been studied for several decades from both theoretical and experimental sides.[1–3] PbTe and PbTe-based alloys doped with group-III (Ga, In, Tl) impurities show interesting properties such as amphoteric nature (both donorlike and acceptorlike behaviors for In), Fermi-surface pinning (for all three), and superconductivity with large T_C (for Tl).[1–4] Due to some of these properties, they have been suggested for highly sensitive far-infrared[3] and terahertz radiation[5] detectors. Functionally graded thermoelectrics based on In-doped PbTe have also been successfully made.[6]

To understand the physical properties of group-III impurities in PbTe, three different models have been proposed in the past.[1] These models are: (i) the "impurity level" model where, for example, In in PbTe forms a localized impurity state which overlaps the conduction band,[7] (ii) the inhomogeneous "mixed-valence" model where In exists in two valence states because In^{2+} valence state is unstable and dissociates into In^{1+} and In^{3+} (i.e., $2In^{2+} \rightarrow In^{1+} + In^{3+}$); the monovalent and trivalent configurations are stabilized by strong electronic and atomic relaxations, modeled by a negative-U Hubbard model,[8–10] and (iii) the "autocompensation" model where two In atoms (rather than 2^+ ions) dissociate into positive and negative charge states (i.e., $2In \rightarrow In^{1+} + In^{1-}$); again the charge states are stabilized by electronic and atomic relaxations.[11]

Although the different proposed models have been quite successful in interpreting several experimental observations, no theoretical justifications to support any or some of these models were available until recently. Extensive studies of the defect states associated with group-III impurities have been carried out using *ab initio* density-functional theory (DFT) and supercell models.[12–16] In these studies, one finds that there are two types of deep defect states. One is a doubly occupied "hyperdeep" defect state (HDS) lying below the bottom of the valence band, more than 5 eV below the Fermi level, and the other is a "deep" defect state (DDS) in the neighborhood of the narrow band gap, where the Fermi level is pinned. Creation of In^{3+} configuration will require taking two electrons from the HDS and putting them near the Fermi energy, a highly energetic event. These studies, therefore, support the impurity level model and suggest that the formation of the trivalent state, hence the coexistence of In^{3+} and In^{1+} configurations, may be difficult energetically. They, however, do not rule out the autocompensation model, which is a different type of mixed-valency in the sense that two In impurities are in 1^+ and 1^- charge states.

Earlier studies of the deep defect states in PbTe have been based mainly on the analysis of electronic density of states.[12–16] The dispersion of the impurity bands, the nature of hybridization of the defect states with the host bands, and the precise position of the impurity levels could not be obtained in those studies because of the overlap of the impurity bands with the PbTe valence and/or conduction bands. In this paper, we present our detailed (**k**-dependence) studies of the impurity bands using supercell models to address these issues and also to understand the relative position of the impurity levels in the dilute impurity limit as one goes from In to Ga to Tl. The arrangement of this paper is as follows. In Sec. II we give some details about our *ab initio* electronic structure calculations. The band structure of undoped PbTe and PbTe doped with Ga, In, and Tl is discussed in Secs. III and IV. We conclude this paper with a summary in Sec. V.

II. CALCULATION METHOD

Structural optimization, total-energy, and electronic structure calculations were performed within the DFT formalism using the generalized-gradient approximation (GGA) (Ref. 17) and the projector-augmented wave[18] (PAW) method as implemented in the VASP code.[19] We treated the outmost s and p electrons of the constituent atoms as valence electrons and the rest as cores (i.e., using the standard PAW potentials

 ©2008 The American Physical Society

in the VASP database). Scalar relativistic effects (mass-velocity and Darwin terms) and spin-orbit interaction (SOI) were included unless otherwise noted. Only scalar relativistic effects were taken into account in structural optimization since it was found that the inclusion of SOI did not have significant influence.[20]

Calculations carried out for undoped and doped PbTe made use of several supercell sizes: primitive cell (2 atoms/cell), $(1\times1\times1)$ unit cell (8 atoms/cell), $(2\times2\times2)$ supercell (64 atoms/cell), and $(3\times3\times3)$ supercell (216 atoms/cell). For the primitive and the unit cells of PbTe, we used $21\times21\times21$ and $11\times11\times11$ Monkhorst-Pack[21] **k**-point meshes, respectively, for the self-consistent run to calculate charge densities, whereas for the $(2\times2\times2)$ and $(3\times3\times3)$ supercells, we used $5\times5\times5$ and $3\times3\times3$ **k**-point meshes, respectively. In all the calculations, the energy cutoff was set to 200 eV and the convergence was assumed when the total-energy difference between cycles was less than 10^{-4} eV. A choice of denser **k**-point meshes and/or larger energy cutoff does not change the physics we are presenting. The optimized lattice constant of undoped PbTe was used to construct the supercells.

III. BAND STRUCTURE OF UNDOPED PbTe

Before introducing the band structure of PbTe doped with group-III (Ga, In, Tl) impurities, we briefly review the band structure of undoped PbTe focusing on the highest valence band and the lowest conduction band. PbTe has NaCl structure with face-centered-cubic (fcc) unit cell. Since a cubic supercell is used in the impurity studies, one needs to know how the band structure of PbTe looks in fcc and cubic Brillouin-zone (BZ) schemes.[22] Let us first discuss this without incorporating SOI. In most of the IV–VI compounds, the valence p states play the dominant role in the formation of the valence and conduction bands. These bands are, respectively, bonding and antibonding states of Pb p and Te p states. The edges of the conduction and valence bands are almost symmetric through the Fermi level and both the maximum and the minimum occur at the same point in the **k** space.[23] In the fcc BZ corresponding to the primitive cell (two atoms/cell; one Pb and one Te), the direct band gap is at the L point [see Fig. 1(a)]. In the absence of SOI, there is a group of six bands (without considering spins) near the band gap at the L point in which three bands (one nondegenerate band and the other twofold degenerate) are above and another three below the Fermi level. We will focus on the two nondegenerate bands, the lowest conduction band and the highest valence band, because they get strongly affected by the impurity when we take into account the fourfold degeneracy associated with four inequivalent L points of the BZ.

Since we are going to work mostly with simple-cubic (sc) BZ, it is important to see how the band structure of PbTe is mapped onto sc BZs with different sizes. In Fig. 1(b) we show the band structure of PbTe along high-symmetry directions of the sc BZ obtained in calculations using a cubic $(1\times1\times1)$ unit cell with eight atoms/cell and a=6.55 Å, the same lattice constant used for the fcc case. It is noted that the sc BZ is (25% in volume) smaller than the fcc BZ. The L

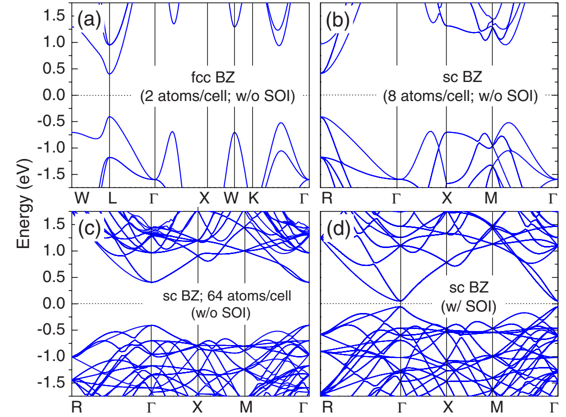

FIG. 1. (Color online) Band structure of undoped PbTe in different Brillouin zones: (a) fcc primitive cell (2 atoms/cell; a=6.55 Å), (b) sc unit cell (8 atoms/cell; a=6.55 Å), (c) sc supercell (64 atoms/cell; a=13.1 Å), and (d) sc supercell (64 atoms/cell; a=13.1 Å) with SOI included. The Fermi level (at 0 eV) is set to the middle of the band gap.

point in the fcc BZ now becomes the R point in the sc BZ and the band extrema occur at R. In a cubic $(2\times2\times2)$ supercell of PbTe with a=13.1 Å (64 atoms/cell), which is eight times larger than the smaller cubic cell, the corresponding BZ is eight times smaller than that for the sc BZ with a=6.55 Å. The band extrema at the R point (of the large sc BZ) now map onto the Γ point of the small sc BZ. We will mostly make use of this small sc BZ (a=13.1 Å) when discussing the effects of group-III impurities on the band structure of PbTe.

Let us now turn our attention to spin-orbit interaction effects and band degeneracies at the valence-band maximum (VBM) and the conduction-band minimum (CBM). There are four inequivalent L points in a fcc BZ. A band which is nondegenerate (disregarding spins) at the L point in the fcc BZ, when mapped into the R (or Γ) point in a sc BZ, becomes fourfold degenerate. This is the case for the CBM and VBM at the R point in the large sc BZ [Fig. 1(b)] or at the Γ point in the smaller sc BZ [Fig. 1(c)]. With spin, the CBM (VBM) at the Γ point [Fig. 1(d)] has eightfold degeneracy. In the presence of SOI, the band gap gets reduced significantly (from 0.816 to 0.105 eV) due to large (0.685 eV) lowering in energy of the Pb p bands (dominant near the conduction-band bottom) and smaller (0.026 eV) change in the Te p bands (dominant near the valence-band top). The calculated band gap (0.105 eV) is much smaller than the experimental value (0.19 eV as $T\to0$ K).[23] This is not surprising since it is well known that DFT-GGA calculations tend to underestimate the band gaps of semiconductors.[27] How the eightfold degeneracy of the CBM and VBM is lifted in the presence of an impurity will be discussed in detail in Sec. IV.

IV. IMPURITY BANDS ASSOCIATED WITH GROUP-III IMPURITIES

We start with a model for group-III substitutional impurities in PbTe using the $(2\times2\times2)$ supercell with the composition $R\,Pb_{n-1}Te_n$ (R=Ga, In, Tl; n=32). The impurity atom

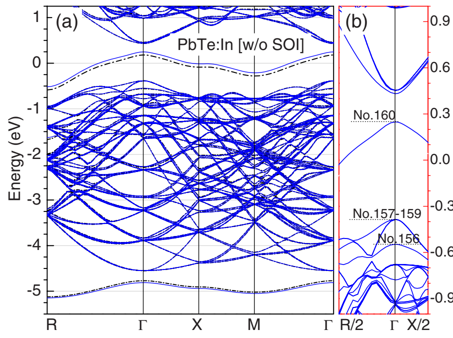

FIG. 2. (Color online) (a) Band structures of In-doped PbTe in calculations using relaxed (solid curves) and unrelaxed (dash-dotted curves) structures, and (b) a blowup of the band structure near the Γ point. The Fermi level for the relaxed structure (at 0 eV) is set to the highest occupied states, whereas that for the unrelaxed one it was shifted by −0.180 eV so that the valence bands match; SOI was not included.

R substitutes the Pb atom at the center of the supercell. The impurity-impurity distance in the $(2\times2\times2)$ supercell is 13.1 Å. In Fig. 2(a) we show the band structure of In-doped PbTe along the high-symmetry directions of the sc BZ obtained with and without atomic relaxation (i.e., allowing for the supercell to relax to its lowest energy structure). For simplicity, the results obtained without SOI are shown in this figure. The impurity bands associated with the HDS and DDS are the nearly flat bands, one at ~ -5 eV and the other in the band-gap region [Fig. 2(a)]. These two bands (denoted as "HDS band" and "DDS band") are the impurity bands associated with In in PbTe. The maxima of the bands are at the Γ point, whereas the minima are at the R point. The HDS and DDS bands resemble each other quite well except that the bandwidth of the HDS band is smaller due the weaker interaction between the neighboring defect states.

A. Atomic relaxation affects the position of the HDS and DDS bands

As can be seen from Fig. 2(a), atomic relaxation rigidly shifts the HDS band away from the valence-band bottom (to lower energy by ~24 meV) and the DDS band away from the valence-band top (to higher energy by ~74 meV) and leaves the remaining bands almost unaffected. For comparison, atomic relaxation in Ga-doped PbTe shifts the HDS and DDS bands in a similar way (i.e., to increase the separation between the two bands) by ~117 and 75 meV, respectively. Atomic relaxation in the case of Tl-doped PbTe, on the other hand, reduces the HDS-DDS distance; the DDS band is shifted down toward the valence-band top by ~27 meV, whereas the HDS is shifted upward toward the valence-band bottom by ~18 meV. This reflects the trend seen after the structural optimization; the neighboring Te atoms move toward Ga (In) impurity and the Ga-Te (In-Te) bond length is decreased by ~2.8% (1.4%), whereas they move away from Tl and the Tl-Te bond length is increased by ~1.4% (also, see Ref. 15). The level repulsion between the impurity bands and the valence band (predominantly Te p) is stronger when the R-Te bond length is shorter.

B. Removal of band degeneracy in the presence of an impurity and the formation of the impurity bands

Let us focus on the region of the **k** space near the Γ point. The topmost occupied band is band 160; this is the DDS band and it is half-filled [Fig. 2(b)]. The HDS band is band 64 and it is filled with two electrons/**k** point. Below it lie 63 bands (31 Pb 6s bands and 32 Te 5s bands) which are also doubly occupied. To understand the parentage of the DDS band, let us first consider the undoped (pure PbTe, i.e., $Pb_{32}Te_{32}$ system) case and look at the number of occupied bands and the degeneracy of the states at $\mathbf{k}=0$ (disregarding the twofold degeneracy of each state; spin degeneracy in the absence of SOI or Kramers degeneracy in the presence of SOI). The VBM and CBM (at Γ) are each fourfold degenerate [Fig. 1(c)]. Here again the topmost filled valence band is the 160th band. These 160 bands come primarily from 32 Pb 6s, 32 Te 5s, and 96 Te 5p orbitals (with some hybridization with Pb p which will be ignored). The total number of 320 valence electrons comes from 128 Pb $6s^26p^2$ and 192 Te $5s^25p^4$ electrons. In the presence of the impurity, these 160 bands undergo drastic rearrangement. The fourfold-degenerate states at the VBM (at Γ) split into nondegenerate (No. 156) and threefold-degenerate (No. 157–159) states. The splitting between these two is ~161 meV. The fourfold-degenerate states at the CBM also split into a nondegenerate and threefold-degenerate states in the presence of the impurity; the splitting is ~22 meV.

It is important to point out that band 160 (the DDS band) is split off neither from the top of the valence band nor from the bottom of the conduction band; it is the result of the strong hybridization between the impurity s state and the entire valence band (predominantly Te p). When In (or Ga, Tl) replaces Pb, one has 319 (=320−4+3) valence electrons in the supercell. Bands 1–159 (which include the HDS) accommodate 318 electrons and the 319th electron occupies the 160th (impurity) band. The DDS band is then half-filled and the Fermi level is pinned in the middle of this band. As long as impurity-impurity interaction (will be discussed later) is weak, the position of the Fermi level does not change with changing the impurity concentration.

To probe the nature of the HDS and DDS bands further, we show in Figs. 3(a) and 3(b) the partial charge densities associated with these two bands in In-doped PbTe. As seen in the figures, the HDS and DDS bands are the bonding and antibonding states of the In 5s and its neighboring Te 5p and are strongly localized within ~6 Å around the impurity atom. The HDS band is predominantly In 5s, whereas the DDS one has more contribution from Te 5p. These strongly localized states are similar to the electrically inactive "hyperdeep level" and the electrically active "deep level" proposed by Hjalmarson *et al.*[24] Partial charge-density analysis also shows that band 156 near the Γ point consists predominantly of states of Te atoms which are the third nearest neighbors of the impurity atom (In), whereas bands 157–159 are predominantly associated with the states of second-nearest-neighbor Te atoms. Also, at the Γ point, the nondegenerate band (No. 161) lying just above the DDS comes from the second-nearest-neighbor Te atoms with some contributions from Pb.

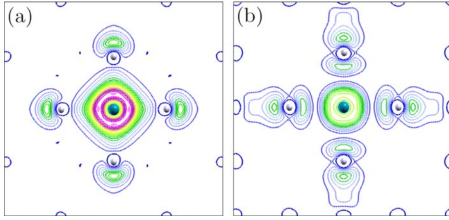

FIG. 3. (Color online) Partial charge densities [in the (100) plane] associated with (a) the HDS and (b) the DDS bands of In-doped PbTe. The results were obtained in calculations using the $(2\times2\times2)$ supercell and without SOI. The isolines in the two figures are plotted with the same scale. Only the impurity atom (large balls at the centers of the figures) and Te (small balls) atoms which are neighbors of the impurity are shown.

The threefold-degenerate bands above it (No. 162–164) come predominantly from Pb states. It is noted that the splittings at the valence-band top and the conduction-band bottom are also present in the absence of local atomic relaxation. They, therefore, are the results of symmetry breaking (and impurity potential) when one replaces a host atom by an impurity.

C. Spin-orbit-induced splittings and hybridization

It is known from Sec. III that SOI has significant effect on the band structure of PbTe, especially on the conduction-band bottom (predominantly Pb *p*) with large spin-orbit-induced downward shift which dramatically reduces the band gap. Since the impurity bands come primarily from the group-III impurity *s* and Te *p* states, one does not expect large spin-orbit-induced shift in these bands. As a result, one expects the dominant hybridization to occur between the conduction band and the impurity band when the conduction bands come down due to SOI.

In Figs. 4(a)–4(c) and 4(a′)–4(c′), we show the band structures of group-III-doped PbTe obtained without and with SOI. In the absence of SOI, the impurity band for In lies primarily in the band gap, except near the *R* point where its minimum lies below the VBM (at Γ). This is also true for Ga and Tl; however, in these two cases, the impurity band lies much closer to the VBM. In the presence of SOI, conduction band comes down and crosses the DDS band; there is hybridization between the DDS band and the conduction band at and near the Γ point [Figs. 4(a′)–4(c′)]. This hybridization strongly distorts both the DDS band and the conduction band in this region. The CBM at the Γ point is now threefold degenerate (sixfold including spins). Partial charge-density analysis, however, shows that the CBM is predominantly Pb; there is very little contribution from the group-III impurity atom to the CBM. The state (which is twofold degenerate) right above the CBM is also predominantly Pb, with very little contribution from the impurity. Above this state, there is another doubly degenerate state (marked by a small circle in the figures) which is, however, predominantly group-III impurity with some mixing with Te *p*. This indicates that, although there are spin-orbit-induced band splittings and hybridization, certain features of the impurity band are still

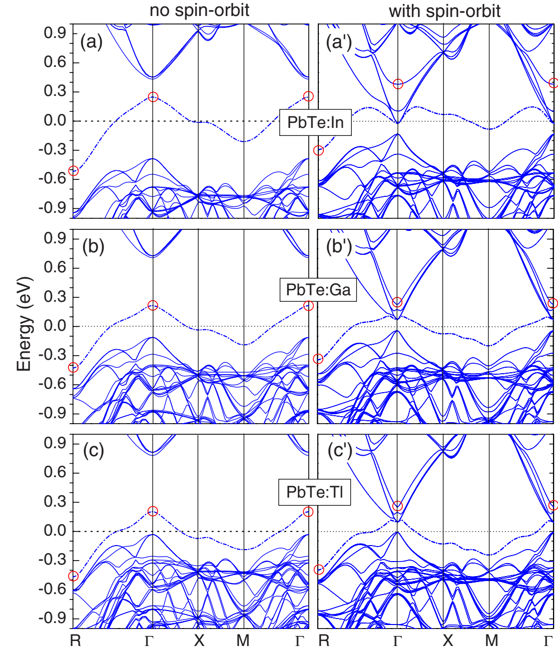

FIG. 4. (Color online) Band structures in the sc BZ of PbTe doped with Ga, In, and Tl impurities in calculations using the $(2\times2\times2)$ supercell and with [(a)–(c)] and without [(a′)–(c′)] SOI. The dash-dotted curves are the DDS bands. The Fermi level (at 0 eV) is set to the highest occupied states.

preserved at an energy level which is close to the original (i.e., without SOI) level at Γ. The CBM (at the Γ point), therefore, is primarily Pb in nature, as in pure PbTe. As a result, one may not be able to experimentally identify the hybridization between the impurity band and the conduction band (in the case of In) for small carrier concentrations. On the other hand, given the fine details of the band structures and the small splittings near the conduction band bottom [Figs. 4(b′) and 4(c′)] and the fact that the band gap of PbTe is underestimated by ~50% in DFT-GGA calculations we speculate that the crossing between the impurity bands associated with Ga and Tl and the conduction band is just an artifact of DFT-GGA.

D. Characteristics of the HDS and DDS bands

To characterize the HDS and DDS bands and see how they are modified by SOI, we summarize in Table I some of their features obtained in calculations with and without SOI. Although these bands have *s* symmetry, SOI has an indirect effect because they have some Te *p* character which is affected by SOI. The bandwidths of the HDS band are slightly increased by SOI by ~4.7% (for Ga), 2.8% (In), and 3.3% (Tl). Both the bandwidth and the change in the bandwidth are monotonic in going from Ga to In to Tl. The distance between the DDS band minima (at *R*) to the band minima which preserves the impurity character; [at Γ; marked by circles in Figs. 4(a′)–4(c′)] is also measured and compared with the DDS bandwidth obtained without SOI. The changes in the DDS band are larger because they have more Te *p* character by ~11.7% (Ga), 12.1% (In), and 3.7% (Tl).

TABLE I. Characteristics of the HDS and DDS bands in group-III-doped PbTe obtained in calculations using the $(2\times2\times2)$ supercell with and without SOI. The bandwidth of the HDS and DDS bands is measured from the minimum at the R point to the maximum at the Γ point [marked by circles in Figs. 4(a)–4(c)]. In the case of DDS with SOI, the bandwidth is measured from the minimum at the R point to the minimum of the band which has the impurity character at the Γ point [marked by circles in Figs. 4(a′)–4(c′)] (see the text). All these quantities are measured in eV.

Band		Ga		In		Tl	
		Band edges	Bandwidth	Band edges	Bandwidth	Band edges	Bandwidth
HDS	Without SOI	$-5.2099(R)$	0.2658	$-5.1472(R)$	0.3352	$-5.4957(R)$	0.3363
		$-4.9441(\Gamma)$		$-4.8120(\Gamma)$		$-5.1594(\Gamma)$	
	With SOI	$-5.2460(R)$	0.2784	$-5.0345(R)$	0.3445	$-5.5145(R)$	0.3475
		$-4.9676(\Gamma)$		$-4.6900(\Gamma)$		$-5.1670(\Gamma)$	
DDS	Without SOI	$-0.4284(R)$	0.6441	$-0.5171(R)$	0.7656	$-0.4692(R)$	0.6728
		$+0.2157(\Gamma)$		$+0.2485(\Gamma)$		$+0.2036(\Gamma)$	
	With SOI	$-0.3443(R)$	0.5693	$-0.2433(R)$	0.6728	$-0.3987(R)$	0.6482
		$+0.2250(\Gamma)$		$+0.3795(\Gamma)$		$+0.2495(\Gamma)$	

E. Impurity levels

The zero of the energy (the Fermi level) in the band structures indicates the average position of the impurity bands associated with the DDS. Since DDS is half-filled and the Fermi level is pinned at the middle of the DDS band, the average band position can be identified as the impurity level. The impurity level associated with In obtained in calculations using the $(2\times2\times2)$ supercell model is ~24 meV above the CBM [Fig. 4(a′)], whereas it is in the band-gap region and ~69 meV below the CBM for Ga [Fig. 4(b′)], and ~5 meV below the VBM for Tl [Fig. 4(c′)]. Scalar relativistic effects (through the Darwin and mass-velocity terms) have strongest effect on the position of the DDS band in the case of Tl ($Z=81$). They push the Tl level below the valence-band top. The impurity levels are, however, anomalous in going from Ga ($Z=31$) to In ($Z=49$) to Tl. This is probably due to the repulsion between Ga s and Pb s since the Ga s level is closest to the Pb s in energy among the three impurities.[25]

In order to pin down the impurity levels further, the band structures for group-III-doped PbTe were calculated using a $(3\times3\times3)$ supercell. This supercell size corresponds to the composition $R\,Pb_{n-1}Te_n$ ($n=108$) and an impurity concentration of ~1%. The large supercell helps reduce the impurity-impurity interaction, thereby, narrowing the width of the HDS and DDS bands. The cubic BZ is now 27 times smaller than the cubic BZ for the $(1\times1\times1)$ cubic cell containing eight atoms. The CBM and VBM are now at the R point [see Figs. 5(a)–5(c)]. Let us denote by $\mathbf{k}^*$ the $\mathbf{k}$ point where the CBM and VBM occur; $\mathbf{k}^*=\{R\}$ in the $(1\times1\times1)$ and $(3\times3\times3)$ cell BZs, whereas $\mathbf{k}^*=\{\Gamma\}$ in the $(2\times2\times2)$ supercell BZ. Note that the Γ-R separation in the BZ of the $(3\times3\times3)$ supercell is one-third that of the $(1\times1\times1)$ cell.

As seen in Figs. 5(a)–5(c) and 5(a′)–5(c′), the impurity bands associated with Ga, In, and Tl in the $(3\times3\times3)$ supercell BZ are very flat (except near the R point). This is consistent with the electronic density-of-states picture obtained in calculations using the same supercell size given earlier where the defect states associated with Ga, In, and Tl gave very sharp peaks.[16] In the presence of SOI, the DDS bands associated with Ga and Tl are decoupled from the conduction-band bottom and have a positive curvature near the R point [see Figs. 5(b′) and 5(c′)]. This supports our speculation made earlier that the crossing between the impurity bands associated with Ga and Tl and the conduction band seen in the calculations using the $(2\times2\times2)$ supercell [Figs. 4(b′) and 4(c′)] is an artifact of DFT-GGA. The DDS band associated with In, however, still has a negative curvature near the $\mathbf{k}$ point where it strongly hybridizes with the conduction-band bottom [see Fig. 5(a′)], similar to what has been observed in the results obtained with the $(2\times2\times2)$ supercell [Fig. 4(a′)].

F. Dilute impurity limit

One of the fundamental questions in the calculation of the energy of a defect state in the dilute (or single impurity) limit using a supercell approach is how to carry out a proper extrapolation in the limit when the size of the supercell goes to infinity. In principle, one can assign a position for the impurity level by averaging the impurity band over the supercell BZ (including $\mathbf{k}^*$).[26] This approach is, however, not practical, e.g., in the current calculations for PbTe using the $(3\times3\times3)$ supercell where one can only compute the band energy at a small number of $\mathbf{k}$ points because of the excessive computational time and computer memory usage (especially when SOI is included). In the following, we will argue that when the impurity-impurity interaction is long ranged (through hybridization or strong mixing with conduction or valence band), it is appropriate to look at $\mathbf{k}$ values which are away from $\mathbf{k}^*$, i.e., large $|\mathbf{k}\text{-}\mathbf{k}^*|$values, and then extrapolate $\mathbf{k}\rightarrow\mathbf{k}^*$.

How the conduction band and the impurity band change as $|\mathbf{k}\text{-}\mathbf{k}^*|\rightarrow0$ is seen clearly by comparing the results for the DDS for In in PbTe as one goes from the $(2\times2\times2)$ supercell [Fig. 4(a′)] to the $(3\times3\times3)$ supercell [Fig. 5(a′)]. Let

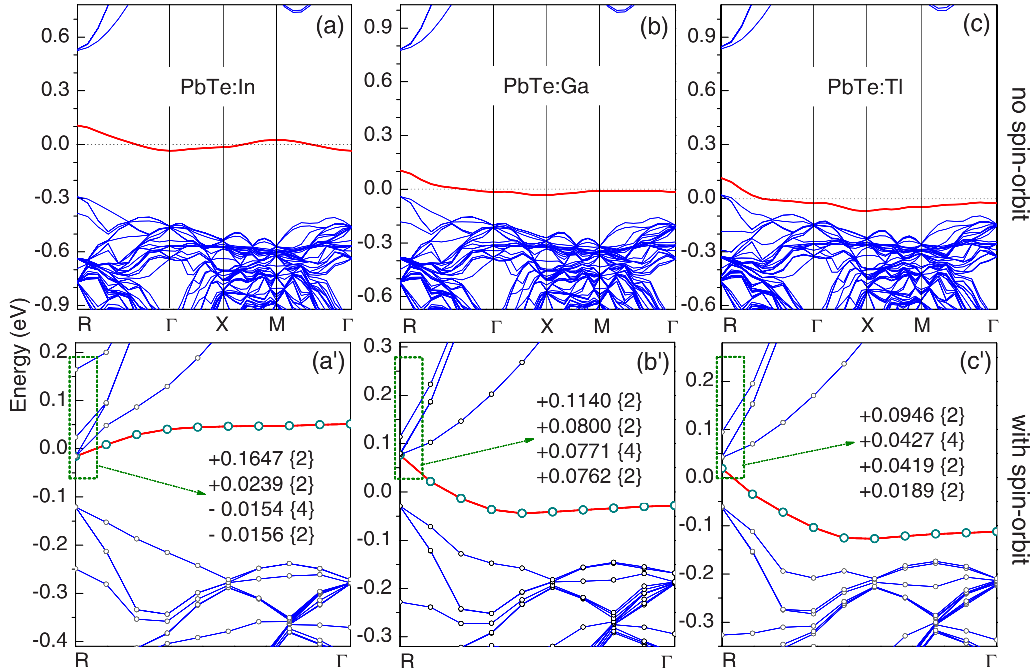

FIG. 5. (Color online) Band structures in the sc BZ of PbTe doped with Ga, In, and Tl impurities obtained in calculations using the $(3\times3\times3)$ supercell and without [(a)–(c)] and with [(a′)–(c′)] SOI. The energy levels near the conduction-band bottom (at the Γ point) are also given in (a′)–(c′) with their respective degeneracies (including spins) in the curly brackets. Note that the zero of energy (the Fermi level) is ill-defined in the results presented in (a′)–(c′) because the calculations scanned only a very small part of the BZ.

us look at the energies between 0 and 0.4 eV at $\mathbf{k}^*=\{\Gamma\}$ for the $(2\times2\times2)$ supercell. The lowest state is nearly sixfold degenerate and ~0.12 eV above it there is a doublet. These eight states are the host conduction-band states (four L point minima with spin degeneracy) which split by the interaction with the impurity. About 0.4 eV above the minimum lies a doublet [marked by a small circle in Fig. 4(a′)] which has a strong impurity character. When we go to the $(3\times3\times3)$ supercell (the band extrema are now at $\mathbf{k}^*=\{R\}$) again we see a nearly sixfold-degenerate state (at −0.015 eV) separated from the next doublet (at +0.024 eV) by ~0.04 eV compared to 0.12 eV in the $(2\times2\times2)$ supercell. The impurity doublet is at 0.165 eV, 0.18 eV above the minimum [compared to ~0.3 eV for the $(2\times2\times2)$ supercell]. So, clearly, there is a strong mixing of the host bands and the impurity state at $\mathbf{k}=\mathbf{k}^*$ in these supercell calculations. The mixing effect goes away as we go to large $|\mathbf{k}\text{-}\mathbf{k}^*|$ values in the $(3\times3\times3)$ supercell. The strong mixing of the impurity band and host band at $\mathbf{k}=\mathbf{k}^*$ is a result of the supercell model. We can now conjecture on a plausible scenario for the single defect limit. The splitting between the lowest sextet and the next doublet goes to zero, recovering the eightfold-degenerate PbTe conduction-band minima. The impurity doublet approaches a limiting value which is the extrapolation of the nearly flat impurity band seen for large $|\mathbf{k}\text{-}\mathbf{k}^*|$.

Based on the above analysis, we estimate the impurity level of In to be ~60 meV above the CBM; for Ga, it is ~100 meV below the CBM, and for Tl, it is ~60 meV below the VBM. These results are in qualitative agreement with experiments where it has been reported that the impurity levels are 70 meV above the conduction-band bottom (in the case of In), 65–70 meV below the conduction-band bottom (for Ga), and about 150–260 meV below the top of the light-hole valence band (for Tl).[2–4] Although the precise position of the DDS with respect to the band edges might not be given accurately by DFT-GGA due to its deficiency in obtaining a correct energy gap,[27] its general structure resulting from hybridization with the host bands, particularly near the band gap, is expected to persist in the real system. Supercell calculations using methods which go beyond GGA, such as screened-exchange local-density approximation[28] and *GW* approximation,[27] may help in determining the accurate position of the impurity levels with respect to the CBM and VBM.

G. Impurity bands in the presence of a stronger impurity-impurity interaction

Until now we have been interested in understanding the nature of defect states in the single or dilute impurity limit. However in many experiments the impurity concentration goes up to 5–6 at. %. This corresponds to one impurity atom for about 16–20 Pb atoms. Even when the impurities are randomly distributed there is a finite possibility that two impurities can come quite close to each other. This will result in strong impurity-impurity interaction.

In order to see how the impurity-impurity interaction affects the impurity bands and their average positions, calculations were carried out using the $(2\times2\times2)$ supercell with (In,In), (Ga,Ga), and (Tl,Tl) substitutional impurity pairs. The composition of the supercell is now $R_2\text{Pb}_{n-2}\text{Te}_n$ ($n=32$) and corresponds to ~6 at. % impurity concentration. The two impurity atoms are either the first, the second, the third, the fourth, or the fifth nearest neighbors of one

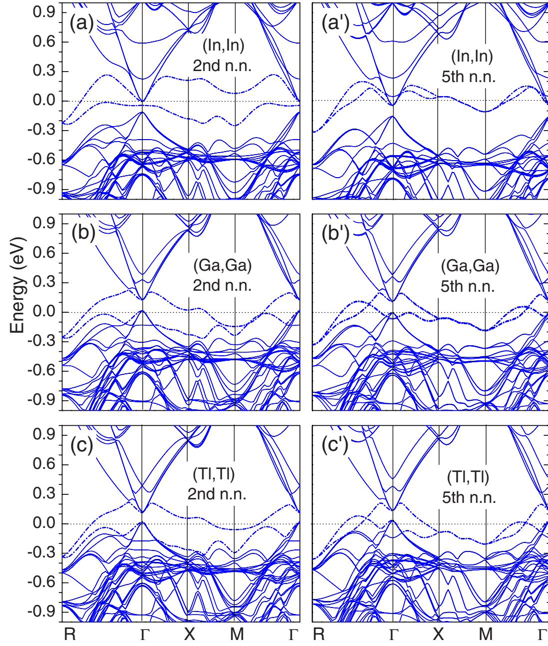

FIG. 6. (Color online) Band splittings due to impurity-impurity interaction in group-III-doped PbTe. The results were obtained in calculations using the $(2\times2\times2)$ supercell with an impurity pair: (In,In) [in (a) and (a′)], (Ga,Ga) [in (b) and (b′)], and (Tl,Tl) [in (c) and (c′)]. The two impurity atoms in a pair are either the second or the fifth nearest neighbors of one another. The dash-dotted curves are the DDS bands. SOI that was included and the Fermi level (at 0 eV) is set to the highest occupied states.

another where the impurity-impurity distances equal to $a/\sqrt{2}$, a, $a\sqrt{3/2}$, $a\sqrt{2}$, and $a\sqrt{3}$, respectively, where a=6.55 Å. Among those five possible pair configurations, the one with the second-nearest neighbors has the lowest energy. This suggests that group-III impurities in PbTe tend to form dimers (through a common Te atom) or In-Te-In chains.[29]

Band structures for the pairs where the two impurities are either the second or the fifth nearest neighbors of one another are shown in Figs. 6(a)–6(c) and 6(a′)–6(c′). In the first case, the impurity-impurity distance is 6.55 Å (before relaxation) with one impurity at the center of the cell. This system can be thought of as a periodic array of In-Te-In chains with interchain separation of 13.10 Å. In the second case, the impurity-impurity distance is 11.35 Å (before relaxation) with one impurity at the center and the other at the corner of the cell. The impurities form a body-centered cubic lattice with unit-cell lattice constant of 13.10 Å. There are now two HDS bands and two DDS bands [see Figs. 6(a)–6(c) and 6(a′)–6(c′)] in the cubic BZ and there are large splittings of the impurity bands due to strong impurity-impurity interaction. In the chain case, the splitting is quite large because the two impurities share a common Te atom. The interaction between the two impurities can be so strong that the resulting splitting can give rise to one resonance state and one bound state. This is clearly seen in Fig. 6(a) where one of the (In) DDS bands lies below the CBM (doubly occupied), whereas the other lies above (unoccupied). In this case, the impurities will not be paramagnetic at low temperatures but will show an almost temperature independent susceptibility, as seen in

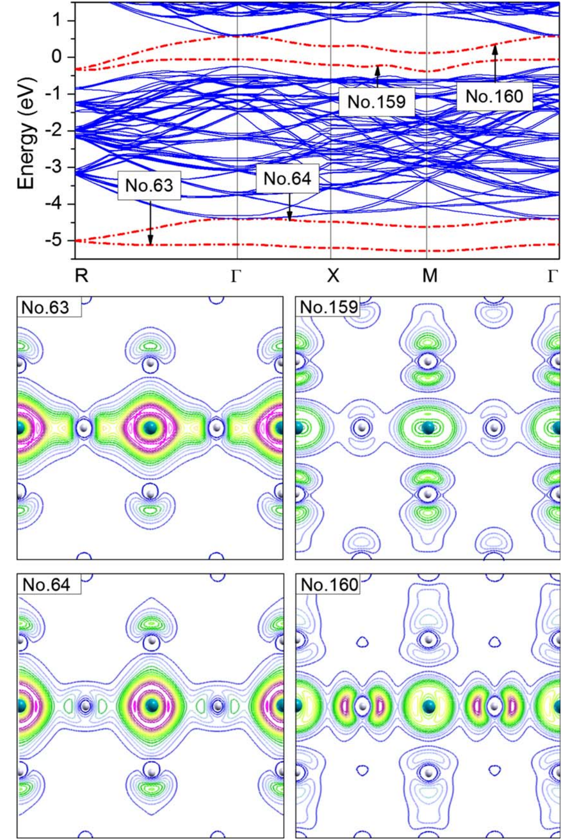

FIG. 7. (Color online) Band structure and partial charge densities associated with the HDS bands [No. 63 and No. 64] and the DDS bands [Nos. 159 and 160] of PbTe doped with (In,In) where the two In atoms in the pair are the second-nearest neighbors of one another. The results were obtained in calculations using the $(2\times2\times2)$ supercell and without SOI. The isolines in the figures were plotted with the same scale. Only the In impurity atoms (large balls) and Te (small balls) atoms which are neighbors of the impurity atoms are shown.

some experiments.[3] For the body-centered cubic geometry, the splitting between the two bands are much smaller. Indium shows a much smaller splitting compared to Ga and Tl, especially at and near the Γ point. This is probably due to the strong hybridization between the DDS bands associated with In and the conduction band. Meanwhile, the crossing between the DDS bands associated with Ga and Tl and the conduction band as seen in Figs. 6(b′) and 6(c′) may be just an artifact of DFT-GGA, as we have mentioned earlier.

In order to visualize the nature of the HDS (DDS) bands in PbTe doped (In,In), we plot in Fig. 7 the band structure showing the two HDS bands and the two DDS bands and their associated partial charge densities. For simplicity, SOI was not included in these calculations. The HDS (DDS) bands are predominantly In s hybridized with Te p states, as seen in the system with one In impurity [Figs. 3(a) and 3(b)]. The charge distribution is, however, strongly modified in the presence of the second In atom, especially along the In-Te-In chain [see also Figs. 3(a) and 3(b) for comparison].

V. SUMMARY

In summary, a careful analysis of the **k** dependence of impurity bands in different supercell sizes has helped in pinning down the position of defect states associated with In, Ga, and Tl impurities in PbTe. In all three systems, there is a deep defect state which lies below the valence band and is doubly occupied. This state, which we call the hyperdeep defect state or HDS, is a bonding state of the *s* state of the impurity and the neighboring Te *p* states. Since it is ~5 eV below the Fermi energy, it will cost a large amount of energy to take two electrons out of this state and place them near the Fermi energy (needed to make In^{3+}). The corresponding antibonding state, which we denote as the deep defect state or DDS, is singly occupied and can be either in the conduction band (for In), in the gap (for Ga), or in the valence band (for Tl). These results are in qualitative agreement with available experimental results.

When two impurity atoms in PbTe are close (for example, in high impurity concentration limit), the strong interaction between the two DDS (HDS) bands associated with these two atoms gives rise to a splitting between them. For In, one DDS band lies below the CBM and is doubly occupied; the other DDS band is unoccupied. In this case, the impurity electrons will be nonmagnetic and will not contribute to Curie susceptibility or electron-spin resonance; this has been seen in some experiments.[3] On the other hand, if the In impurities are far apart then the DDS will be degenerate, each impurity having one electron. In this case, the impurities will be paramagnetic contributing to Curie susceptibility and electron-spin resonance. However, it is possible that one electron from one impurity DDS is transferred to the DDS of another impurity that is already occupied with one electron. This charge-transfer state can be stabilized by a negative Hubbard U. In this case, both the impurity sites will not be paramagnetic. This is the essence of the autocompensation model (where, e.g. $2In^0 \rightarrow In^{1+} + In^{1-}$).[11]

ACKNOWLEDGMENTS

This work was partially supported by the MURI under Grant No. N00014–03–10789 from the Office of Naval Research. Calculations were performed at the High Performance Computing Center of Michigan State University.

*Present address: Materials Department, University of California, Santa Barbara, California 93106-5050, USA.
†Corresponding author. mahanti@pa.msu.edu

[1] K. Lischka, Appl. Phys. A: Solids Surf. **A29**, 177 (1982).
[2] S. A. Nemov and Yu. I. Ravich, Phys. Usp. **41**, 735 (1998).
[3] B. A. Volkov, L. I. Ryabova, and D. R. Khokhlov, Phys. Usp. **45**, 819 (2002).
[4] Y. Matsushita, H. Bluhm, T. H. Geballe, and I. R. Fisher, Phys. Rev. Lett. **94**, 157002 (2005).
[5] D. R. Khokhlov, Phys. Usp. **49**, 955 (2006).
[6] Z. Dashevsky, S. Shusterman, M. P. Dariel, and I. Drabkin, J. Appl. Phys. **92**, 1425 (2002).
[7] A. A. Averkin, V. I. Kaidanov, and R. B. Mel'nik, Sov. Phys. Semicond. **5**, 75 (1971).
[8] Yu. V. Andreev, K. I. Geimann, I. A. Dabkin, A. V. Matveenko, E. A. Mozhaev, and B. Ya. Moizhes, Sov. Phys. Semicond. **9**, 1235 (1976).
[9] I. A. Drabkin and B. Ya. Moĭzhes, Sov. Phys. Semicond. **15**, 357 (1981).
[10] B. A. Volkov and O. M. Ruchaĭskiĭ, JETP Lett. **62**, 217 (1995).
[11] K. Weiser, A. Klein, and M. Ainhorn, Appl. Phys. Lett. **34**, 607 (1979).
[12] S. Ahmad, K. Hoang, and S. D. Mahanti, Phys. Rev. Lett. **96**, 056403 (2006).
[13] S. Ahmad, S. D. Mahanti, K. Hoang, and M. G. Kanatzidis, Phys. Rev. B **74**, 155205 (2006).
[14] I. Hase and T. Yanagisawa, Physica C **445-448**, 61 (2006).
[15] K. Hoang, S. D. Mahanti, and P. Jena, Phys. Rev. B **76**, 115432 (2007).
[16] S. D. Mahanti, K. Hoang, and S. Ahmad, Physica B **401-402**, 291 (2007).
[17] J. P. Perdew, K. Burke, and M. Ernzerhof, Phys. Rev. Lett. **77**, 3865 (1996).
[18] P. E. Blöchl, Phys. Rev. B **50**, 17953 (1994); G. Kresse and D. Joubert, *ibid.* **59**, 1758 (1999).
[19] G. Kresse and J. Hafner, Phys. Rev. B **47**, 558 (1993); G. Kresse and J. Hafner, *ibid.* **49**, 14251 (1994); G. Kresse and J. Furthmüller, *ibid.* **54**, 11169 (1996); G. Kresse and J. Furthmüller, Comput. Mater. Sci. **6**, 15 (1996).
[20] L. E. Ramos, L. K. Teles, L. M. R. Scolfaro, J. L. P. Castineira, A. L. Rosa, and J. R. Leite, Phys. Rev. B **63**, 165210 (2001).
[21] H. J. Monkhorst and J. D. Pack, Phys. Rev. B **13**, 5188 (1976).
[22] M. Lax, *Symmetry Principles in Solid State and Molecular Physics* (Wiley, New York, 1974).
[23] *Lead Chalcogenides: Physics and Applications*, edited by D. Khokhlov (Taylor & Francis, New York, 2003).
[24] H. P. Hjalmarson, P. Vogl, D. J. Wolford, and J. D. Dow, Phys. Rev. Lett. **44**, 810 (1980).
[25] The energy levels are −12.49 (Pb *s*), −11.55 (Ga *s*), −10.14 (In *s*), and −9.83 (Tl *s*); see, W. A. Harrison, *Elementary Electronic Structure* (World Scientific, Singapore, 2004).
[26] R. M. Nieminen, in *Theory of Defects in Semiconductors*, edited by D. A. Drabold and S. Estreicher (Springer, Berlin, 2007).
[27] W. G. Aulber, L. Jonsson, and J. W. Wilkins, Solid State Phys. **54**, 1 (2000).
[28] D. M. Bylander and L. Kleinman, Phys. Rev. B **41**, 7868 (1990).
[29] The total energies (without SOI) of, e.g., $In_2Pb_{30}Te_{32}$ are −238.2531, −238.3154, −238.2179, −238.2104, and −238.2095 eV for the first, second, third, fourth, and fifth nearest-neighbor pair configurations, respectively.